European Journal of Medicinal Chemistry 80 (2014) 47–56

Contents lists available at ScienceDirect

European Journal of Medicinal Chemistry

journal homepage: http://www.elsevier.com/locate/ejmech

Original article

Synthesis, biological evaluation, molecular docking and theoretical evaluation of ADMET properties of nepodin and chrysophanol derivatives as potential cyclooxygenase (COX-1, COX-2) inhibitors

Jagdeep Grover [a], Vivek Kumar [b], Vikram Singh [a], Khemraj Bairwa [a], M. Elizabeth Sobhia [b], Sanjay M. Jachak [a,*]

[a] Department of Natural Products, National Institute of Pharmaceutical Education and Research, Sector-67, S.A.S. Nagar, 160062 Punjab, India
[b] Department of Pharmacoinformatics, National Institute of Pharmaceutical Education and Research, Sector-67, S.A.S. Nagar, 160062 Punjab, India

ARTICLE INFO

Article history:
Received 28 September 2013
Received in revised form
3 March 2014
Accepted 10 April 2014
Available online 13 April 2014

Keywords:
Nepodin
Chrysophanol
COX inhibitors
Anti-inflammatory
Molecular docking

ABSTRACT

Nepodin and chrysophanol, isolated from *Rumex nepalensis* roots, showed significant cyclooxygenase (COX) inhibitory activity. To further optimize these lead molecules and study structure activity relationship (SAR), eighteen derivatives of nepodin and nine derivatives of chrysophanol were synthesized and evaluated for COX-1 and COX-2 inhibitory potential. Among the synthesized compounds, four nepodin (**1f**, **1g**, **1h** and **1i**) and three chrysophanol (**2e**, **2f** and **2h**) derivatives displayed more pronounced COX-2 inhibition than their respective lead molecule. Further, compounds **1f**, **1g**, **2e** and **2h** exhibited better anti-inflammatory activity than ibuprofen in carrageenan-induced rat paw edema assay. Taking into account the *in vitro* and *in vivo* results, molecular docking and *in silico* prediction of ADMET properties of compounds were carried out respectively.

1. Introduction

Cyclooxygenase (COX) or prostaglandin endoperoxide synthase (PGHS), exists in two isoforms, COX-1 and COX-2. COX-1 is constitutively expressed in a variety of cell types and is mainly involved in the synthesis of cytoprotective PGs in gastrointestinal (GI) tract, whereas COX-2 is inducible and its expression is induced during inflammatory conditions, provoked by pro-inflammatory molecules such as IL-1, TNF-α, LPS and TPA [1–3]. Several reports revealed that inhibition of COX-1 by classical NSAIDs is associated with unfavorable GI side effects such as gastrointestinal ulcers, bleeding, and platelet dysfunction, which led to the hypothesis that selective COX-2 inhibitors (coxibs) might be endowed with improved anti-inflammatory properties and reduced gastrointestinal toxicity profiles than classical NSAIDs. This hypothesis was validated in both animal models and human clinical trials that lead to the development of coxibs as a new generation NSAIDs. But, on the other hand serious cardiovascular adverse events have been reported in some trials of coxibs [4,5]. Therefore, development of better anti-inflammatory molecules with improved COX-1/COX-2 selectivity index is a need of hour.

Natural products have engrossed substantial attention for the management of inflammation as NSAIDs possess certain side effects. Reported anti-inflammatory natural products belong to different chemical classes such as alkaloids, steroids, terpenoids, polyphenolics, phenylpropanoids, fatty acids and lipids [6]. Recently, we have reported that the ethyl acetate extract of *Rumex nepalensis* roots exhibited significant COX-1 and COX-2 inhibition. Further, the extract was also evaluated in TPA-induced acute inflammation mouse model and significant reduction in ear edema was observed. HPLC analysis of *R. nepalensis* roots revealed presence of two major compounds, which were isolated and characterized as nepodin (**1**) and chrysophanol (**2**, Fig. 1). These compounds were evaluated for COX inhibition *in vitro*. Nepodin exhibited significant inhibition of COX-1 and COX-2 whereas, chrysophanol was found to inhibit COX-2 moderately [7,8]. Chrysophanol and its derivatives have also been reported to possess anticancer activity [9]. Inspired by the aforesaid findings, and as a part of our ongoing program to discover COX-1 and COX-2 inhibitory compounds from Indian medicinal plants [10–12], we aimed to synthesize derivatives of **1** and **2** to optimize these lead molecules and study structure activity relationship (SAR). Chemically, nepodin

* Corresponding author.
E-mail addresses: sanjayjachak@niper.ac.in, sjachak11@gmail.com (S.M. Jachak).

http://dx.doi.org/10.1016/j.ejmech.2014.04.033
0223-5234/

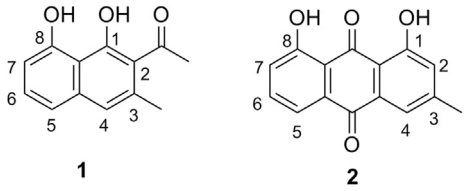

Fig. 1. Chemical structure of nepodin and chrysophanol.

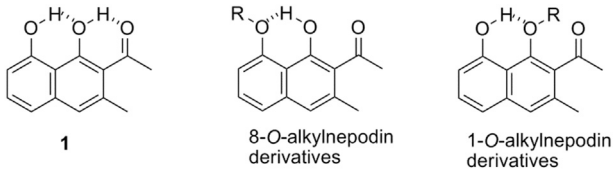

Fig. 2. Hydrogen bonding in nepodin and its derivatives.

posessess naphthalene skeleton with two hydroxyl groups at C-1 and C-8, and an acetyl group at C-2. Two hydrogen bonds (HBs) also exits in structure of **1**; one involving acetyl oxygen and neighboring hydroxyl group and another between oxygen atoms at 1 and 8 positions (Fig. 2). ^{1}H NMR of **1** displaying, the hydroxyl group at C-1 and C-8 at δ 17.35 and 10.23 ppm respectively, indicated the environmental influence on the nature of two HBs [7,13]. Although no studies have been carried out in the past to study the nature of hydrogen bonding in **1**, but the same has been studied in another structurally similar compound, 2-acetyl-1,8-dihydroxy-3,6-dimethylnaphthalene. The study explained that these HBs are of different strength and electronic nature. The interaction between an acetyl oxygen and 1-OH group is a short and strong covalent interaction, whereas the other involving oxygen centers at 1 and 8 positions is normal electrostatic HB [14,15]. It can be inferred that similar electronic strength of HBs may also exist in **1**. Hence, these two hydroxyl groups possessing different chemical environment can be targeted to study SAR.

2. Results and discussion

2.1. Chemistry

Nepodin (**1**) and chrysophanol (**2**) were isolated from ethyl acetate extract of *R. nepalensis* roots. Chemical modifications of **1** were carried out at 1- and 8-OH groups to introduce different functionalities (Scheme 1). It was observed that in each reaction, regioselective alkylation took place at 8-OH, whereas 1-*O*-alkylated products were formed in less yields. This difference in the extent of reaction at C-1 and C-8 hydroxyl groups can be rationalized owing to difference in the strength of two HBs as discussed above. Because of weak HB at 8-OH, nucleophilic substitution occurred more promptly at this position as compared to at 1-OH position, as expected. Moreover, the nature of HB was also studied in both regioisomers. From IR and NMR study, it was observed that carbonyl group is non-chelated in both the isomers. The carbonyl group appears at 1674–1694 cm^{-1} in case of 8-*O*-alkyl and 1-*O*-alkyl derivatives, whereas it appears at 1631 cm^{-1} in case of **1**. In 8-*O*-alkyl derivatives, hydroxyl group at C-1 appears at δ 9.73–10.23 ppm in ^{1}H NMR, confirming that the proton of 1-OH is hydrogen bonded to oxygen atom at C-8, and not with carbonyl group at C-2 (Fig. 2).

In case of chrysophanol (**2**), strength of HB is same for both hydroxyl groups at C-1 and C-8, as observed from ^{1}H NMR chemical shift of these hydroxyl groups [7] and, hence these groups were substituted with different functionalities to study the effect of substitution on activity (Scheme 2). Of the total 27 synthesized compounds, 25 were found to be new as per scifinder and reaxys database search.

2.2. Biological evaluation

2.2.1. In vitro inhibition of COX

All the prepared nepodin and chrysophanol derivatives (**1a–i, 1a′–i′** and **2a–i**) were evaluated for *in vitro* COX-1 and COX-2 inhibitory potential in a COX-catalyzed prostaglandin biosynthesis assay at 30 μM concentration [7,10]. Four nepodin (**1f–i**) and three chrysophanol derivatives (**2e**, **2f** and **2h**) showed significant COX-1 and COX-2 inhibitory activity. The study was further extended to determine IC_{50} values of seven active compounds (Table 1). Compound **1g** demonstrated highest COX-2 inhibition (IC_{50} 11.21 μM) followed by **1h** (12.17 μM) and **1i** (14.23 μM). Aromatic substitution (**1g**, **1h** and **1i**) was a determinant of the COX-2 inhibitory potency and selectivity. Within aromatic substitution, it was observed that **1h** displayed highest COX-2 selectivity (SI = 2.01), followed by **1i** (SI = 1.56) and **1g** (SI = 1.35), which might be due to larger size of bromine in **1h**. Among Chrysophanol derivatives, compound **2e** showed highest COX-2 inhibition (IC_{50} = 11.64 μM) followed by **2h** (IC_{50} = 16.81 μM) and **2f** (IC_{50} = 20.01 μM).

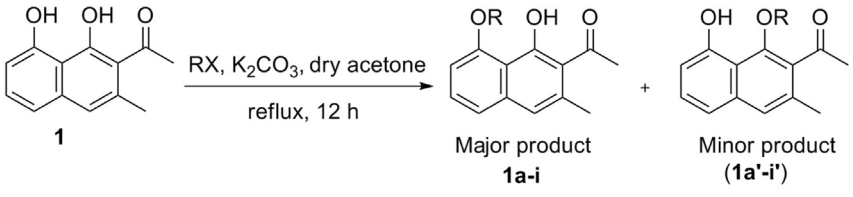

RX	R	Compound
CH_3I	CH_3	**1a**, **1a'**
$BrCH_2CH_3$	CH_2CH_3	**1b**, **1b'**
$BrCH_2CH_2CH_3$	$CH_2CH_2CH_3$	**1c**, **1c'**
$BrCH_2CH_2CH_2CH_3$	$CH_2CH_2CH_2CH_3$	**1d**, **1d'**
$(CH_3)_2CHBr$	$(CH_3)_2CH$	**1e**, **1e'**
$ClCH_2OCH_3$	CH_2OCH_3	**1f**, **1f'**
$BrCH_2C_6H_5$	$CH_2C_6H_5$	**1g**, **1g'**
$2\text{-}BrCH_2C_6H_4Br$	$2\text{-}BrCH_2C_6H_4$	**1h**, **1h'**
$3\text{-}ClCH_2C_6H_4Br$	$3\text{-}ClCH_2C_6H_4$	**1i**, **1i'**

Scheme 1. Synthesis of 8- and 1-*O*-alkylether derivatives of nepodin.

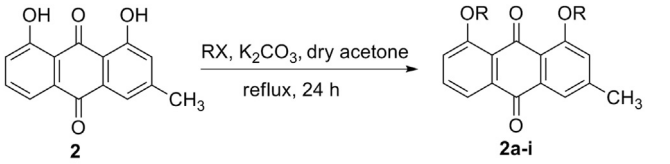

RX	R	Compound
CH_3I	CH_3	**2a**
$BrCH_2CH_3$	CH_2CH_3	**2b**
$BrCH_2CH_2CH_3$	$CH_2CH_2CH_3$	**2c**
$BrCH_2CH_2CH_2CH_3$	$CH_2CH_2CH_2CH_3$	**2d**
CH_2=$CHCH_2Br$	CH_2=$CHCH_2$	**2e**
$BrCH_2C_6H_5$	$CH_2C_6H_5$	**2f**
3-$ClCH_2C_6H_4Br$	3-$ClCH_2C_6H_4$	**2g**
4-$ICH_2C_6H_4Br$	4-$ICH_2C_6H_4$	**2h**
2-$BrCH_2C_6H_4Br$	2-$BrCH_2C_6H_4$	**2i**

Scheme 2. Synthesis of 1,8-dialkylether derivatives of chrysophanol.

Moreover, to signify the effect of bulkiness on biological evaluation, COX inhibition was correlated with taft steric substituent constant E_s [16]. E_s represents the bulkiness of substituent and, values for different substituents are listed in Table 1. As mentioned above, different COX inhibition results were observed with aliphatic and aromatic substitution. COX inhibition of compounds (**1a**–**d**, **1a**′–**d**′ and **2a**–**d**) decreased significantly with increasing bulkiness of alkyl chain ($E_s = -0.39$ for butyl substituent, compound **1d**, **1d**′ and **2d**). However, an isopropyl substituent retains activity ($E_s = -0.47$, compound **1e** and **1e**′). In contrast, bulkiness of aromatic substituent (**1g**–**i**, **1g**′–**i**′ and **2f**–**i**) positively influenced COX inhibition and was a determinant of COX-2 inhibitory potency. Within aromatic substitution, increasing the bulkiness at *ortho* position of aromatic ring resulted in enhanced COX-2 selectivity (**1h, SI = 2.01**). Similar results were observed for other compounds (**1g**, **1i** and **2f**–**i**). Therefore it can be stated that steric effect contributes significantly toward the COX inhibition, although not in a same manner for aliphatic and aromatic substitution.

2.2.2. *In vivo assay*

Seven compounds (**1f**–**i**, **2e**, **2f** and **2h**) that showed potent COX inhibition *in vitro*, were further evaluated for *in vivo* anti-inflammatory activity (AI) at a dose of 150 μmol/kg in carrageenan-induced rat paw edema assay. Carrageenan-induced edema is a non-specific inflammation resulting from a complex of diverse mediators. This assay has been used for investigating new anti-inflammatory agents, since it reliably predicts the anti-inflammatory efficacy of the NSAIDs [17]. The investigated compounds exhibited moderate to good anti-inflammatory activity with the percentage inhibition of edema ranged from 37.0 to 55.8 at 5 h, while the reference drug ibuprofen demonstrated 43.5% inhibition at 5 h (Table 2). Compound **2f** and **1h** exhibited comparable activity, whereas compound **1f**, **1g**, **2e** and **2h** showed better activity, than ibuprofen.

Based on the above observations we propose a SAR as below:

Nepodin derivatives (i) Introduction of chain length up to four carbons (**1a**–**d** and **1a**′–**d**′) resulted in a decreased COX-1 and COX-2 inhibitory activity. However, an isopropyl group at 8-position (**1e**)

Table 1
In vitro COX-1 and COX-2 inhibitory activities of nepodin and chrysophanol derivatives.

Compound	COX inhibition at 30 μM[a]		(IC_{50}, μM)		SI[c]	E_s[d] (substituent)
	COX-1	COX-2	COX-1	COX-2		
1a	69.8 ± 0.31	61.7 ± 1.19	ND	ND	ND	0 ($-CH_3$)
1a′	65.5 ± 0.21	55.5 ± 0.34	ND	ND	ND	0 ($-CH_3$)
1b	62.1 ± 0.27	54.2 ± 1.01	ND	ND	ND	−0.07 ($-C_2H_5$)
1b′	58.4 ± 1.21	42.9 ± 0.10	ND	ND	ND	−0.07 ($-C_2H_5$)
1c	53.5 ± 0.67	35.4 ± 0.19	ND	ND	ND	−0.36 ($-(CH_2)_2CH_3$
1c′	51.4 ± 0.81	47.0 ± 0.76	ND	ND	ND	−0.36 ($-(CH_2)_2CH_3$
1d	28.5 ± 2.11	31.9 ± 1.10	ND	ND	ND	−0.39 ($-(CH_2)_3CH_3$
1d′	40.2 ± 1.33	37.9 ± 0.60	ND	ND	ND	−0.39 ($-(CH_2)_3CH_3$
1e	70.9 ± 0.08	62.6 ± 0.32	ND	ND	ND	−0.47 ($-CH(CH_3)_2$
1e′	62.2 ± 0.17	54.9 ± 2.10	ND	ND	ND	−0.47 ($-CH(CH_3)_2$
1f	80.6 ± 0.09	75.0 ± 1.49	17.2	19.01	0.9	NF
1f′	67.1 ± 0.63	61.5 ± 0.43	ND	ND	ND	NF
1g	83.4 ± 0.53	89.9 ± 1.01	15.21	11.21	1.35	−0.38 ($-CH_2Ph$)
1g′	60.2 ± 1.47	68.2 ± 0.99	ND	ND	ND	−0.38 ($-CH_2Ph$)
1h	63.6 ± 2.17	83.1 ± 1.45	24.47	12.17	2.01	NF
1h′	37.2 ± 0.71	67.5 ± 2.08	ND	ND	ND	NF
1i	67.1 ± 1.62	82.1 ± 0.88	22.23	14.23	1.56	NF
1i′	34.9 ± 1.55	64.9 ± 0.23	ND	ND	ND	NF
2a	59.2 ± 0.12	62.1 ± 0.94	ND	ND	ND	0 ($-CH_3$)
2b	43.7 ± 0.38	55.5 ± 1.2	ND	ND	ND	−0.07 ($-C_2H_5$)
2c	39.6 ± 1.29	58.7 ± 0.66	ND	ND	ND	−0.36 ($-(CH_2)_2CH_3$
2d	26.0 ± 2.39	42.0 ± 1.22	ND	ND	ND	−0.39 ($-(CH_2)_3CH_3$
2e	44.3 ± 1.71	81.5 ± 1.09	>30	11.64	>2.57	NF
2f	41.4 ± 1.81	76.5 ± 0.73	>30	20.01	>1.49	−0.38 ($-CH_2Ph$)
2g	25.4 ± 0.24	61.0 ± 1.44	ND	ND	ND	NF
2h	64.2 ± 0.82	77.8 ± 0.54	>30	16.81	>1.78	NF
2i	27.23 ± 1.19	62.0 ± 0.15	ND	ND	ND	NF
1	68.24 ± 0.98	59.42 ± 0.32	27.43	32.28	0.84	
2	29.37 ± 0.73	42.12 ± 0.13	46.21	36.12	1.27	
Indomethacin[b]	98.2 ± 0.33	51.0 ± 0.34	0.18	>30	ND	
Celecoxib[b]	13.0 ± 0.63	95.6 ± 0.48	>30	0.15	>200	

ND – not determined, NF – not found.
[a] Values are expressed as mean ± SEM of three determinations ($n = 3$).
[b] Positive control used.
[c] Selectivity index (COX-1 IC_{50}/COX-2 IC_{50}).
[d] Values from ref 16.

Table 2
In vivo acute anti-inflammatory activity of nepodin and chrysophanol derivatives in carrageenan-induced rat paw edema assay at dose 150 μmol/kg.

Compound	Anti-inflammatory activity	
	% Inhibition after 3 h ± SEM	% Inhibition after 5 h ± SEM
1f	36.4 ± 1.49*	55.8 ± 2.54*
1g	30.3 ± 1.17*	54.2 ± 3.65*
1h	25.5 ± 1.57*	46.5 ± 1.21*
1i	26.6 ± 1.57*	37.0 ± 0.93*
2e	35.6 ± 2.57*	50.9 ± 1.76*
2f	28.2 ± 2.13*	45.1 ± 2.83*
2h	36.1 ± 3.67*	54.6 ± 3.70*
ibuprofen	32.3 ± 1.26*	43.5 ± 1.47*

The results are expressed as mean ± SEM ($n = 5$). Significance was calculated by using one-way ANOVA with Dunnet's *t*-test. The difference in results were considered significant when $p < 0.05$. *$p < 0.001$ vs. control.

did not alter COX-1 and COX-2 inhibition. (ii) Substitution of 8-OH with methoxymethylene group (**1f**) leads to enhanced COX-1 and COX-2 inhibition and exhibited significant AI activity. (iii) The compounds with bulkier substituents such as benzyl (**1g**), 2-bromobenzyl (**1h**) and 3-chlorobenzyl (**1i**) on 8-OH displayed enhanced COX-2 selectivity (Fig. 3A). (iv) The 8-*O*-alkyl derivatives showed comparatively better COX-1 and COX-2 inhibition as compared to 1-*O*-alkyl derivatives.

Similar results were observed in case of chrysophanol derivatives (*v*) Increasing the carbon chain length up to four carbons (**2a**–**d**) decreased COX-1 and COX-2 inhibitory activity. (vi) Replacement of 1- and 8-OH with allyl group (**2e**) enhanced COX-2 inhibition, whereas COX-1 inhibition was not increased significantly. (vii) Substitution of 1- and 8-OH with bulkier groups like benzyl (**2f**), 3-chlorobenzyl (**2g**), 4-iodobenzyl (**2h**) and 2-bromobenzyl (**2i**) enhanced COX-2 inhibition (Fig. 3B). This observed COX-2 selectivity could be due to larger volume of COX-2 enzyme that can accommodate bulkier groups.

2.3. Molecular docking studies

Molecular docking study was carried out to predict binding mode and orientation of compounds at the active sites of COX-1 and COX-2. GOLD program successfully docked compound **1**, **2** and their derivatives into the active sites of COX-1 and COX-2 enzyme. The residues involved in HB interactions during complex formation and their Gold fitness scores are summarized in Table 3. Gold fitness score was observed reasonably higher for some of the nepodin (**1g**, **1g′**, **1h**, **1h′**, **1i** and **1i′**) and chrysophanol derivatives (**2a**–**i**) against COX-2. Selectivity of these compounds towards COX-2 may be attributed to increase in bulkiness of substituent group, which is rationalized by large binding pocket of COX-2 that can ably accommodate bulky compounds in its binding cavity. 8-*O*-

Table 3
Gold fitness scores of nepodin and chrysophanol derivatives and HBs formed with amino acid residues of COX-1 and COX-2.

Compounds	Gold fitness score COX-1	Residues of COX-1 involved in HB interactions	Gold fitness score COX-2	Residues of COX-2 involved in HB interactions
1	38.39	Ser530	38.64	Ser530
1a	38.98	Ser530	38.35	–
1a′	38.90	Ala527	38.01	–
1b	37.15	Ser530	39.46	–
1b′	35.75	Ser530	39.06	Ser530
1c	35.21	Ser530	38.18	Ala527
1c′	35.30	Ser530	39.52	Tyr355
1d	21.22	Ser530	37.36	Tyr355
1d′	26.39	Ser530	38.79	Tyr355
1e	41.62	Ala527	41.26	Ala527
1e′	37.02	Ser530	36.70	–
1f	44.79	Ala527	43.22	Ala527
1f′	39.79	Ser530, Tyr385	39.37	Ser530
1g	43.91	Ser530	54.36	Ser530
1g′	34.54	Ser530	44.00	Tyr355
1h	40.23	Ser530	49.43	Tyr355, Arg 120
1h′	26.38	Ser530	51.99	Tyr355
1i	43.42	Ser530	46.35	Tyr355
1i′	29.48	Ser530	46.82	Tyr355
2	48.54	Ser530, Met522	51.98	Ser530
2a	49.29	Ser530	51.89	Ser530
2b	35.44	Ser530	47.77	Ser530
2c	33.32	Ser530	50.59	Ser530
2d	27.78	Ser530	36.95	Ser530
2e	33.64	Ser530	51.62	Ser530
2f	32.36	Ser530	47.98	Ser530
2g	17.74	Ser530	32.35	Ser530
2h	41.60	Ser530	46.13	Ser530
2i	25.00	Ser530	36.26	Ser530

Alkylated nepodin derivatives demonstrated higher gold score against COX-1 and COX-2 as compared to 1-*O*-alkylated nepodin derivatives, corroborating *in vitro* data. These compounds were observed to form HB interactions with residues Tyr355, Met522, Ala527 and Ser530 into the active site of COX-1, while with residues Arg 120, Tyr355, Ala527 and Ser530 in COX-2. However, frequency of H-bond interaction of examined compounds was found higher for Ser530 in COX-1, while for Tyr355, Ala527 and Ser530 in COX-2. The interaction with amino acid Ser530 is important for COX inhibitory activity and is well exemplified by the binding interaction of aspirin with COX-1 and COX-2 [18]. This indicated the importance of residue Ser530 for inhibition of the COX-1 and COX-2, in addition to residues Tyr355 and Ala527 for selective inhibition of COX-2.

The most potent compound **1g** was found to dock into the active site of COX-1 with GOLD fitness score of 43.91 (Fig. 4A1). It formed one HB with residue Ser530 and bonding distance of 2.61Å was observed between –CanithaO of **1g** and OH of Ser530 (H … O). The

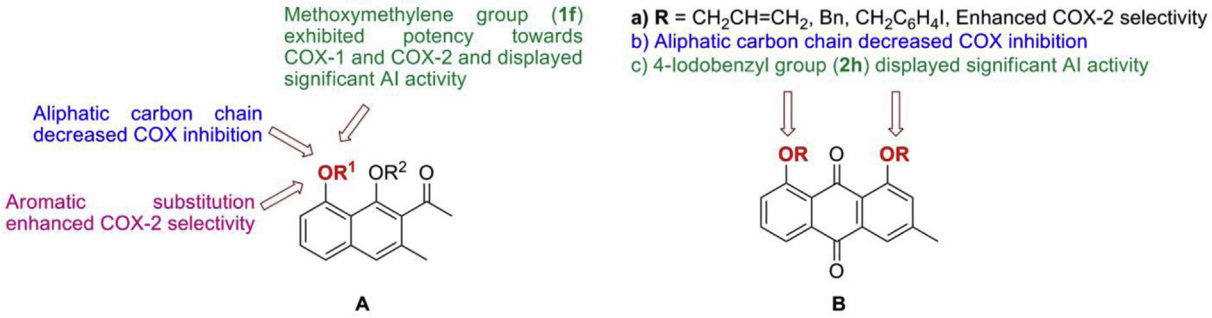

Fig. 3. Structure activity relationship of nepodin (A) and chrysophanol (B) derivatives.

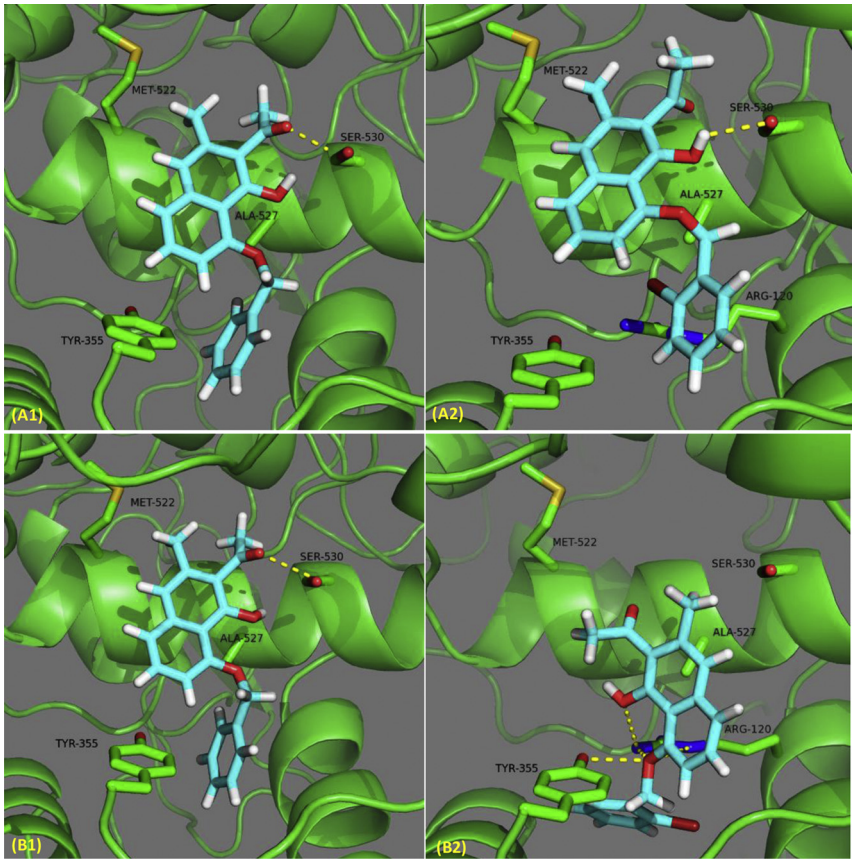

Fig. 4. Binding mode of compound **1g** and **1h** at the active site of COX-1 (A1 and A2) and COX-2 (B1 and B2) respectively.

2-CanithaO, 3-Me, 1-OH and 8-Bn of **1g** were surrounded by the active site amino acid residues Ser530, Met522, Ala527 and Tyr355 respectively. However, it docked into the active site of COX-2 with GOLD fitness score of 54.36 (Fig. 4B1). It formed one HB in COX-2 with residues Ser530 with bonding distance of 2.90 Å between –CanithaO of **1g** and OH of Ala527 (O … H). The naphthalene and benzyl ring of **1g** was surrounded by the similar active site amino acid residues as in case of COX-1. The comparable GOLD fitness score of **1g** against both COX-1 and COX-2 rationalized its non-selectivity which was also in coherence with experimental enzyme inhibition. Compound **1h** docked into the active site of COX-1 with GOLD fitness score of 40.23 (Fig. 4A2). One HB between 1-OH of **1h** and OH of Ser530 (H … O, 2.5 Å) was observed. The 3-Me, 1-OH, 8-OCH_2 and phenyl ring (attached to OCH_2) of **1h** were surrounded by the active site amino acid residues Met522, Ser530, Ala527 and Arg 120 respectively. It successfully docked into the active site of COX-2 as well with GOLD fitness score of 49.43 (Fig. 4B2). Three hydrogen bonding interactions of **1h** were observed with the bonding distances as follow: 1-OH of **1h** and NH of Arg 120 (O … HN, 1.9 Å), 8-O of **1h** and OH of Tyr355 (O … H, 1.9 Å) and 8-O of **1h** and NH of Arg 120 (O … HN, 2.9 Å). The 3-Me, 2-$COCH_3$, naphthalene and phenyl ring of **1h** were surrounded by the active site amino acid residues Ser530, Met522, Ala527 and Arg 120, and Tyr355 respectively. Similar results were observed for compounds **2a**–**i**. Compound **2e** showed highest GOLD fitness score against COX-2 (51.62). It was also noted that both COX-1 and COX-2 share almost similar active site residues and difference lies in its active site volume (COX-2 has larger active site volume-417 Å; while COX-1 has smaller active site volume-366 Å) [3]. Only difference was observed at position 523 where COX-1 and COX-2 contain isoleucine and valine respectively (Fig. 5). The additional methyl group at Ile523 in COX-1 was reported to obstruct ligand gating into side pocket of COX-1. However, this side pocket was easily accessible in case of COX-2, facilitating the accommodation of bulkier groups [3,19].

2.4. Theoretical evaluation of ADMET properties

Most active compounds (**1f**–**i**, **2e**, **2f** and **2h**) were evaluated for the ADMET properties *in silico* using the Accelrys Discovery Studio

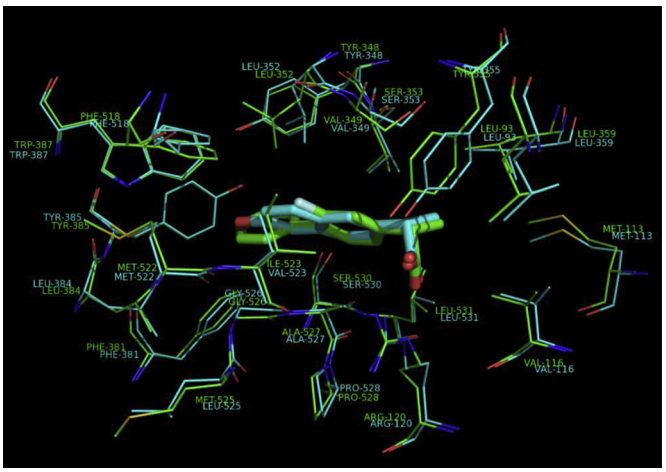

Fig. 5. Superimposition of binding site residues of COX-1 (green) and COX-2 (cyan). (For interpretation of the references to colour in this figure legend, the reader is referred to the web version of this article.)

(Table 4). Compounds **1f**–**i** showed ADMET properties similar to drugs flurbiprofen and celecoxib. These compounds (**1f**–**i**) were predicted to have good absorption, high blood brain barrier (BBB) and good solubility, comparable with standard drugs. In addition, the compounds **1f**, **1g** and **1i** followed Lipinski's rule of five (molecular weight, log P, number of hydrogen donors and acceptors). However, the compounds **1g**–**i** showed a vast probability of hepatotoxicity (>0.92), whereas **1f** showed hepatotoxicity probability of 0.52, less than flurbiprofen and celecoxib. The studied compounds showed significant enzyme inhibition against COX-1 and COX-2, however, only compound **1f** showed a good ADMET profile similar to naproxen. It is evident that these compounds have potential to inhibit COX enzyme, however, they need to be optimized further for their pharmacokinetics properties.

3. Conclusion

In summary, eighteen nepodin and nine chrysophanol derivatives were screened for *in vitro* COX inhibitory activity. From SAR study, we successfully demonstrated that compounds with bulkier substitutions (**1g**, **1h**, **1i**, **2e**, **2f** and **2h**) were more selective towards COX-2. These molecules were further evaluated for anti-inflammatory activity *in vivo*. Four compounds (**1f**, **1g**, **2e a**nd **2h**) displayed better anti-inflammatory activity than ibuprofen. Molecular docking study helped in supporting the observed COX-1 and COX-2 activity profiles. Most active compounds displayed good oral absorption, solubility and lipophilicity when evaluated for ADMET properties *in silico*. Compound **1f** demonstrated good ADMET profile similar to naproxen with least probability of hepatotoxicity. Aforementioned findings inferred **1f** as a potential COX inhibitor and anti-inflammatory agent and thus render it as a lead molecule for further development of new anti-inflammatory agents with better pharmacokinetic properties.

4. Experimental

4.1. Materials and equipments

All Chemicals were purchased from Sigma Aldrich. Melting points were determined on a PERFIT digital melting point apparatus. ^{1}H and ^{13}C NMR spectra were recorded in deuterated solvents on Bruker 400 Ultra Shield™ NMR spectrophotometer with TMS as an internal standard. High resolution mass spectra were recorded on MaXis™ UHR-TOF. IR spectra were recorded on Nicolet FT-IR (Impact 410, Japan) spectrophotometer.

4.2. General method for the preparation of ether derivatives of nepodin and chrysophanol

A conventional method of *O*-alkylation using potassium carbonate (K_2CO_3) as a base in aprotic solvent was used. To a stirred solution of **1** (0.69 mmol) containing potassium carbonate (1.17 mmol) in dry acetone (8–10 mL), an appropriate alkylating agent (1.04 mmol) was added dropwise and resulting reaction mixture was refluxed for 15–24 h. Progress of reaction was monitored by TLC. On completion, the reaction was quenched with water and aqueous portion was extracted with EtOAc (3 × 30 mL). Organic layer was passed over anhydrous Na_2SO_4 and solvent was removed under vacuum. The crude product was purified by CC (hexane/ethylacetate 98:2) to give desired 1- and 8-*O*-alkylated nepodin derivatives. Similar procedure was followed for the preparation of chrysophanol derivatives using 4 equiv of both potassium carbonate and alkylating agents.

4.2.1. 1-(1-Hydroxy-8-methoxy-3-methylnaphthalen-2-yl) ethanone (**1a**)

Brown solid. Yield 72%. mp: 95–97 °C. ^{1}H NMR (400 MHz, $CDCl_3$) δ (ppm): 2.33 (s, 3H, Ar–CH_3), 2.62 (s, 3H, $COCH_3$), 4.03 (s, 3H, OCH_3), 6.73 (dd, 1H, J = 7.0, 1.6 Hz, H-7), 7.07 (s, 1H, H-4), 7.25–7.33 (m, 2H, H-5, H-6), 9.73 (s, 1H, OH). ^{13}C NMR (100 MHz, $CDCl_3$) δ: 20.0, 32.2, 56.1, 104.0, 113.2, 119.7, 121.1, 124.6, 127.0, 134.1, 136.6, 152.4, 156.5, 205.5. IR (KBr, cm^{-1}) 3364, 2917, 1673. HRMS (ESI) *m/z*: Calcd for $C_{14}H_{14}O_3Na$ $[M + Na]^+$ 253.0841; found 253.0839.

4.2.2. 1-(8-Hydroxy-1-methoxy-3-methylnaphthalen-2-yl) ethanone (**1a′**)

Brown solid. Yield 23%. mp: 83–85 °C. ^{1}H NMR (400 MHz, $CDCl_3$) δ (ppm): 2.36 (s, 3H, Ar–CH_3), 2.62 (s, 3H, $COCH_3$), 3.93 (s, 3H, OCH_3), 6.88 (dd, 1H, J = 7.64 0.92, Hz, H-7), 7.24–7.26 (m, 1H, H-5), 7.38 (t, 1H, J = 7.85 Hz, H-6), 7.42 (s, 1H, H-4), 9.14 (s, 1H, OH). ^{13}C NMR (100 MHz, $CDCl_3$) δ: 19.4, 32.5, 65.1, 110.5, 115.0, 118.6, 125.8, 128.7, 131.5, 132.1, 136.5, 153.1, 153.7, 205.0. IR (KBr, cm^{-1}) 3418, 2917, 1694. HRMS (ESI) *m/z*: Calcd for $C_{14}H_{14}O_3Na$ $[M + Na]^+$ 253.0841; found 253.0839.

4.2.3. 1-(8-Ethoxy-1-hydroxy-3-methylnaphthalen-2-yl)ethanone (**1b**)

Brown solid. Yield 70%. mp: 98–101 °C. ^{1}H NMR (400 MHz, $CDCl_3$) δ (ppm): 1.60 (t, 3H, J = 7 Hz, CH_3), 2.38 (s, 3H, Ar–CH_3), 2.65 (s, 3H, $COCH_3$), 4.32 (q, 2H, J = 12.76, 6.96 Hz, CH_2), 6.75 (dd, 1H, J = 6.44, 2.24 Hz, H-7), 7.10 (s, 1H, H-4), 7.28–7.34 (m, 2H, H-5, H-6), 9.93 (s, 1H, OH); ^{13}C NMR (100 MHz, $CDCl_3$) δ: 14.7, 19.9, 32.3, 65.2, 104.8, 113.2, 119.7, 120.9, 124.6, 127.0, 134.0, 136.6, 152.4, 155.8,

Table 4
Theoretical prediction of ADMET properties of selected nepodin and chrysophanol derivatives.[a]

Compound	Log P	Molecular weight	HBA	HBD	Rot_Bond	PSA	BBB Level[d]	Absorption_ Level[e]	Log *S*[c]	Heptox_Probability	PPB[b]
1f	2.557	260.285	3	1	4	55.76	2	0	−3.31	0.529	2
1g	4.289	306.355	2	1	4	46.53	1	0	−5.016	0.953	1
1h	5.037	385.251	2	1	4	46.53	1	0	−5.815	0.927	2
1i	4.954	340.8	2	1	4	46.53	1	0	−5.73	0.96	1
2e	5.577	335.373	4	0	6	77.68	0	0	−6.447	0.768	2
2f	6.428	434.483	4	0	6	52.6	4	1	−7.382	0.986	2
2h	7.585	686.276	4	0	6	52.6	4	3	−8.342	0.986	2
Flurbiprofen	3.68	244.26	2	1	3	37.29	1	0	−4.08	0.61	2
Naproxen	2.84	230.25	3	1	3	46.53	2	0	−3.56	0.48	2
Celecoxib	4.42	381.37	3	1	4	86.36	2	0	−6.6	0.85	1

[a] The data was determined with Accelrys Discovery Studio.
[b] PPB, Plasma protein binding (0 = PPB < 90% and 2 = PPB > 95%).
[c] Log *S* < −8.0 = extreme low, Log *S* −6.0 < 2.0 = good.
[d] BBB, Blood brain barrier (0 = very high and 3 = low).
[e] Absorption_level (0 = good and 3 = very low).

205.5. IR (KBr, cm^{-1}) 3300, 2922, 1676. HRMS (ESI) *m/z*: Calcd for $C_{15}H_{16}O_3Na$ $[M + Na]^+$ 267.0997; found 267.0991.

4.2.4. 1-(1-Ethoxy-8-hydroxy-3-methylnaphthalen-2-yl)ethanone (**1b′**)

Brown solid. Yield 27%. mp: 87–88 °C. ^1H NMR (400 MHz, $CDCl_3$) δ (ppm): 1.45 (t, 3H, $J = 7.08$ Hz, CH_3), 2.35 (s, 3H, Ar–CH_3), 2.63 (s, 3H, $COCH_3$), 4.11 (q, 2H, $J = 14.12$, 7.04 Hz, CH_2), 6.86 (dd, 1H, $J = 7.64$, 0.84, Hz, H-7), 7.23–7.26 (m, 1H, H-5), 7.38 (t, 1H, H-6, $J = 7.96$ Hz), 7.41 (s, 1H, H-4), 9.35 (s, 1H, OH). ^{13}C NMR (100 MHz, $CDCl_3$) δ: 15.3, 19.5, 32.5, 74.8, 110.3, 115.5, 118.5, 125.6, 128.6, 131.6, 132.1, 136.4, 152.0, 153.9, 205.2. IR (KBr, cm^{-1}) 3365, 2930, 1691. HRMS (ESI) *m/z*: Calcd for $C_{15}H_{16}O_3Na$ $[M + Na]^+$ 267.0997; found 267.0989.

4.2.5. 1-(1-Hydroxy-3-methyl-8-propoxynaphthalen-2-yl) ethanone (**1c**)

Brown solid. Yield 65%. mp: 73–75 °C. ^1H NMR (400 MHz, $CDCl_3$) δ (ppm): 1.12 (t, 3H, $J = 7.44$ Hz, CH_3), 1.94–1.99 (m, 2H, CH_2), 2.35 (s, 3H, Ar–CH_3), 2.61 (s, 3H, $COCH_3$), 4.18 (t, 2H, $J = 6.48$ Hz, OCH_2), 6.73 (dd, 1H, $J = 6.56$, 2.12 Hz, H-7), 7.08 (s, 1H, H-4), 7.26–7.32 (m, 2H, H-5, H-6), 9.90 (s, 1H, OH). ^{13}C NMR (100 MHz, $CDCl_3$) δ: 10.5, 19.9, 22.4, 32.3, 71.1, 104.7, 113.2, 119.7, 120.9, 124.6, 127.0, 134.0, 136.6, 152.4, 155.9, 205.6. IR (KBr, cm^{-1}) 3298, 2935, 1689. HRMS (ESI) *m/z*: Calcd for $C_{16}H_{18}O_3Na$ $[M + Na]^+$ 281.1154; found 281.1153.

4.2.6. 1-(8-Hydroxy-3-methyl-1-propoxynaphthalen-2-yl) ethanone (**1c′**)

Brown solid. Yield 30%. mp: 68–69 °C. ^1H NMR (400 MHz, $CDCl_3$) δ (ppm): 1.04 (t, 3H, $J = 7.40$ Hz, CH_3), 1.82–1.89 (m, 2H, CH_2), 2.35 (s, 3H, Ar–CH_3), 2.62 (s, 3H, $COCH_3$), 3.99 (t, 2H, $J = 6.8$ Hz, OCH_2), 6.86 (dd, 1H, $J = 7.60$, 0.52 Hz, H-7), 7.23–7.26 (m, 1H, H-5), 7.37 (t, 1H, H-6, $J = 7.96$ Hz), 7.40 (s, 1H, H-4), 9.32 (s, 1H, OH). ^{13}C NMR (100 MHz, $CDCl_3$) δ: 10.1, 19.4, 23.1, 32.7, 80.7, 110.2, 115.4, 118.5, 125.6, 128.6, 131.6, 132.1, 136.5, 152.1, 153.9, 205.2. IR (KBr, cm^{-1}) 3364, 2927, 1690. HRMS (ESI) *m/z*: Calcd for $C_{16}H_{18}O_3Na$ $[M + Na]^+$ 281.1154; found 281.1147.

4.2.7. 1-(8-Butoxy-1-hydroxy-3-methylnaphthalen-2-yl)ethanone (**1d**)

Brown solid. Yield 60%. mp: 64–65 °C. ^1H NMR (400 MHz, $CDCl_3$) δ (ppm): 1.02 (t, 3H, $J = 7.36$ Hz, CH_3), 1.50–1.60 (m, 2H, CH_2), 1.88–1.95 (m, 2H, CH_2), 2.35 (s, 3H, Ar–CH_3), 2.61 (s, 3H, $COCH_3$), 4.21 (t, 2H, $J = 6.48$ Hz, OCH_2), 6.72 (dd, 1H, $J = 6.48$, 2.12 Hz, H-7), 7.07 (s, 1H, H-4), 7.25–7.31 (m, 2H, H-5, H-6), 9.88 (s, 1H, OH). ^{13}C NMR (100 MHz, $CDCl_3$) δ: 13.7, 19.2, 19.9, 31.0, 32.3, 69.3, 104.7, 113.3, 119.7, 120.9, 124.6, 127.0, 134.0, 136.6, 152.4, 156.0, 205.5. IR (KBr, cm^{-1}) 3313, 2922, 1674. HRMS (ESI) *m/z*: Calcd for $C_{17}H_{20}O_3Na$ $[M + Na]^+$ 295.1310; found 295.1325.

4.2.8. 1-(1-Butoxy-8-hydroxy-3-methylnaphthalen-2-yl)ethanone (**1d′**)

Brown solid. Yield 30%. mp: 62–63 °C. ^1H NMR (400 MHz, $CDCl_3$) δ (ppm): 1.00 (t, 3H, $J = 7.36$ Hz, CH_3), 1.45–1.54 (m, 2H, CH_2), 1.81–1.88 (m, 2H, CH_2), 2.37 (s, 3H, Ar–CH_3), 2.64 (s, 3H, $COCH_3$), 4.05 (t, 2H, $J = 6.84$ Hz, OCH_2), 6.88 (dd, 1H, $J = 7.60$, 0.76 Hz, H-7), 7.25–7.28 (m, 1H, H-5), 7.39 (t, 1H, $J = 7.96$ Hz H-6), 7.42 (s, 1H, H-4), 9.35 (s, 1H, OH). ^{13}C NMR (100 MHz, $CDCl_3$) δ: 13.7, 18.9, 19.4, 31.9, 32.6, 79.1, 110.2, 115.4, 118.5, 125.6, 128.6, 131.6, 132.0, 136.5, 152.1, 153.9, 205.2. IR (KBr, cm^{-1}) 3365, 2935, 1692. HRMS (ESI) *m/z*: Calcd for $C_{17}H_{20}O_3Na$ $[M + Na]^+$ 295.1310; found 295.1330.

4.2.9. 1-(1-Hydroxy-8-isopropoxy-3-methylnaphthalen-2-yl) ethanone (**1e**)

Yellow solid. Yield 69%. mp: 68–69 °C. ^1H NMR (400 MHz, $CDCl_3$) δ (ppm): 1.53 (d, 6H, $J = 6.08$ Hz, $2CH_3$), 2.37 (s, 3H, Ar–CH_3), 2.65 (s, 3H, $COCH_3$), 4.85–4.89 (m, 1H, O–CH), 6.79 (dd, 1H, $J = 7.16$, 1.32 Hz, H-7), 7.09 (s, 1H, H-4), 7.28–7.35 (m, 2H, H-5, H-6), 10.13 (s, 1H, OH). ^{13}C NMR (100 MHz, $CDCl_3$) δ: 19.9, 22.0, 32.3, 72.8, 106.3, 114.0, 119.6, 120.8, 124.5, 127.0, 134.0, 136.7, 152.5, 154.5, 205.6. IR (KBr, cm^{-1}) 3434, 2923, 1672. HRMS (ESI) *m/z*: Calcd for $C_{16}H_{18}O_3Na$ $[M + Na]^+$ 281.1154; found 281.1185.

4.2.10. 1-(8-Hydroxy-1-isopropoxy-3-methylnaphthalen-2-yl) ethanone (**1e′**)

Yellow solid. Yield 26%. mp: 61–62 °C. ^1H NMR (400 MHz, $CDCl_3$) δ (ppm): 1.35 (d, 6H, $J = 6.16$ Hz, $2CH_3$), 2.37 (s, 3H, Ar–CH_3), 2.65 (s, 3H, $COCH_3$), 4.38–4.44 (m, 1H, O–CH), 6.86 (dd, 1H, $J = 7.64$, 0.64 Hz, H-7), 7.23–7.25 (m, 1H, H-5), 7.38 (t, 1H, H-6, $J = 8$ Hz), 7.41 (s, 1H, H-4), 9.55 (s, 1H, OH). ^{13}C NMR (100 MHz, $CDCl_3$) δ: 19.7, 21.8, 32.1, 82.0, 110.3, 117.0, 118.2, 125.4, 128.7, 131.1, 132.2, 136.2, 151.0, 154.3, 205.5. IR (KBr, cm^{-1}) 3365, 2939, 1691. HRMS (ESI) *m/z*: Calcd for $C_{16}H_{18}O_3Na$ $[M + Na]^+$ 281.1154; found 281.1186.

4.2.11. 1-(1-Hydroxy-8-(methoxymethoxy)-3-methylnaphthalen-2-yl)ethanone (**1f**)

Yellow solid. Yield 57%. mp: 52–54 °C. ^1H NMR (400 MHz, $CDCl_3$) δ (ppm): 2.39 (s, 3H, Ar–CH_3), 2.65 (s, 3H, $COCH_3$), 3.59 (s, 3H, OCH_3), 5.44 (s, 2H, OCH_2), 7.02 (dd, 1H, $J = 7.32$, 1.24 Hz, H-7), 7.12 (s, 1H, H-4), 7.28–7.37 (m, 2H, H-5, H-6), 9.77 (s, 1H, OH). ^{13}C NMR (100 MHz, $CDCl_3$) δ: 20.0, 32.2, 56.9, 95.8, 107.7, 113.5, 119.9, 122.0, 124.7, 127.1, 134.0, 136.6, 152.1, 154.0, 205.4. IR (KBr, cm^{-1}) 3365, 2937, 1691. HRMS (ESI) *m/z*: Calcd for $C_{15}H_{16}O_4Na$ $[M + Na]^+$ 283.0946; found 283.0959.

4.2.12. 1-(8-Hydroxy-1-(methoxymethoxy)-3-methylnaphthalen-2-yl)ethanone (**1f′**)

Yellow solid. Yield 34%. mp: 49–50 °C. ^1H NMR (400 MHz, $CDCl_3$) δ (ppm): 2.38 (s, 3H, Ar–CH_3), 2.66 (s, 3H, $COCH_3$), 3.55 (s, 3H, OCH_3), 5.17 (s, 2H, OCH_2), 6.92 (d, 1H, $J = 7.64$ Hz, H-7), 7.26–7.39 (m, 2H, H-5, H-6), 7.44 (s, 1H, H-4), 9.10 (s, 1H, OH). ^{13}C NMR (100 MHz, $CDCl_3$) δ: 19.5, 32.6, 58.9, 103.7, 110.9, 115.7, 118.6, 126.0, 128.7, 132.0, 132.7, 136.4, 149.6, 153.8, 205.1. IR (KBr, cm^{-1}) 3360, 2923, 1692. HRMS (ESI) *m/z*: Calcd for $C_{15}H_{16}O_4Na$ $[M + Na]^+$ 283.0946; found 283.0973.

4.2.13. 1-(8-(benzyloxy)-1-hydroxy-3-methylnaphthalen-2-yl) ethanone (**1g**)

White solid. Yield 65%. mp: 67–68 °C. ^1H NMR (400 MHz, $CDCl_3$) δ (ppm): 2.37 (s, 3H, Ar–CH_3), 2.59 (s, 3H, $COCH_3$), 5.28 (s, 2H, OCH_2), 6.86 (d, 1H, $J = 7.7$ Hz, H-7), 7.11 (s, 1H, H-4), 7.32–7.49 (m, 7H, Ar–H), 9.73 (s, 1H, OH). ^{13}C NMR (100 MHz, $CDCl_3$) δ: 19.9, 32.2, 71.7, 105.1, 119.7, 121.3, 126.8, 127.9, 128.0, 128.1, 128.4, 128.9, 129.1, 134.1, 135.0, 152.1, 155.7, 205.6. IR (KBr, cm^{-1}) 3230, 2921, 1672. HRMS (ESI) *m/z*: Calcd for $C_{20}H_{18}O_3Na$ $[M + Na]^+$ 329.1154; found 329.1158.

4.2.14. 1-(1-(benzyloxy)-8-hydroxy-3-methylnaphthalen-2-yl) ethanone (**1g′**)

White solid. Yield 25%. mp: 69–70 °C. ^1H NMR (400 MHz, $CDCl_3$) δ (ppm): 2.41 (s, 3H, Ar–CH_3), 2.67 (s, 3H, $COCH_3$), 5.01 (s, 2H, OCH_2), 6.90 (d, 1H, $J = 7.56$ Hz, H-7), 7.29–7.50 (m, 8H, Ar–H), 9.19 (s, 1H, OH). ^{13}C NMR (100 MHz, $CDCl_3$) δ: 19.4, 32.9, 81.0, 110.5, 118.6, 125.9, 127.9, 128.5, 128.6, 128.9, 129.2, 129.3, 129.4, 132.0, 134.5, 136.5, 151.3, 153.6, 205.4. IR (KBr, cm^{-1}) 3393, 2923, 1685. HRMS (ESI) *m/z*: Calcd for $C_{20}H_{18}O_3Na$ $[M + Na]^+$ 329.1154; found 329.1159.

*4.2.15. 1-(8-(2-Bromobenzyloxy)-1-hydroxy-3-methylnaphthalen-2-yl)ethanone (**1h**)*

White solid. Yield 60%. mp: 153–155 °C. ^{1}H NMR (400 MHz, $CDCl_3$) δ (ppm): 2.38 (s, 3H, Ar–CH_3), 2.61 (s, 3H, $COCH_3$), 5.40 (s, 2H, OCH_2), 6.83 (dd, 1H, J = 5.88, 2.76 Hz, H-7), 7.12 (s, 1H, H-4), 7.27–7.38 (m, 4H, Ar–H), 7.53 (dd, 1H, J = 7.60, 1.36 Hz, Ar–H), 7.67 (dd, 1H, J = 7.96, 0.92 Hz, Ar–H), 9.70 (s, 1H, OH). ^{13}C NMR (100 MHz, $CDCl_3$) δ: 20.0, 32.3, 71.1, 105.4, 113.3, 119.8, 121.5, 123.3, 127.0, 128.0, 130.0, 130.4, 133.2, 134.1, 134.3, 136.7, 152.3, 155.4, 205.5. IR (KBr, cm^{-1}) 3364, 2917, 1691. HRMS (ESI) *m/z*: Calcd for $C_{20}H_{17}BrO_3Na$ $[M + Na]^+$ 407.0259; found 407.0259.

*4.2.16. 1-(1-(2-Bromobenzyloxy)-8-hydroxy-3-methylnaphthalen-2-yl)ethanone (**1h′**)*

White solid. Yield 33%. mp: 123–125 °C. ^{1}H NMR (400 MHz, $CDCl_3$) δ (ppm): 2.38 (s, 3H, Ar–CH_3), 2.63 (s, 3H, $COCH_3$), 5.13 (s, 2H, OCH_2), 6.88 (d, 1H, J = 7.6 Hz, H-7), 7.27–7.65 (m, 7H, Ar–H), 8.94 (s, 1H, OH). ^{13}C NMR (100 MHz, $CDCl_3$) δ: 19.4, 33.0, 67.0, 110.6, 115.4, 118.7, 120.8, 123.6, 126.1, 127.3, 128.6, 130.5, 132.0, 132.2, 133.1, 134.5, 136.5, 151.4, 153.5, 205.2. IR (KBr, cm^{-1}) 3366, 2917, 1673. HRMS (ESI) *m/z*: Calcd for $C_{20}H_{17}BrO_3Na$ $[M + Na]^+$ 407.0259; found 407.0259.

*4.2.17. 1-(8-(3-Chlorobenzyloxy)-1-hydroxy-3-methylnaphthalen-2-yl)ethanone (**1i**)*

White solid. Yield 63%. mp: 93–95 °C. ^{1}H NMR (400 MHz, $CDCl_3$) δ (ppm): 2.37 (s, 3H, Ar–CH_3), 2.61 (s, 3H, $COCH_3$), 5.24 (s, 2H, OCH_2), 6.80 (dd, 1H, J = 6.64, 2.0 Hz, H-7), 7.12 (s, 1H, H-4), 7.27–7.47 (m, 6H, Ar–H), 9.66 (s, 1H, OH). ^{13}C NMR (100 MHz, $CDCl_3$) δ: 19.9, 32.2, 70.9, 105.4, 113.3, 119.8, 121.6, 124.9, 125.9, 126.9, 128.0, 129.1, 130.4, 134.2, 134.9, 136.7, 137.0, 152.1, 155.4, 205.4. IR (KBr, cm^{-1}) 3330, 2930, 1672. HRMS (ESI) *m/z*: Calcd for $C_{20}H_{17}ClO_3Na$ $[M + Na]^+$ 363.0764; found 363.0766.

*4.2.18. 1-(1-(3-Chlorobenzyloxy)-8-hydroxy-3-methylnaphthalen-2-yl)ethanone (**1i′**)*

White solid. Yield 30%. mp: 78–80 °C. ^{1}H NMR (400 MHz, $CDCl_3$) δ (ppm): 2.40 (s, 3H, Ar–CH_3), 2.66 (s, 3H, $COCH_3$), 4.97 (s, 2H, OCH_2), 6.90 (dd, 1H, J = 6.12, 2.35 Hz, H-7), 7.31–7.48 (m, 7H, Ar–H), 8.99 (s, 1H, OH). ^{13}C NMR (100 MHz, $CDCl_3$) δ: 19.0, 32.9, 70.7, 107.7, 110.7, 118.8, 121.1, 125.0, 125.8, 127.0, 127.5, 127.8, 128.7, 129.0, 129.4, 130.2, 136.5, 150.7, 153.4, 205.4. IR (KBr, cm^{-1}) 3362, 2915, 1690. HRMS (ESI) *m/z*: Calcd for $C_{20}H_{17}ClO_3Na$ $[M + Na]^+$ 363.0764; found 363.0766.

*4.2.19. 1,8-Dimethoxy-3-methylanthracene-9,10-dione (**2a**)*

Yellow solid. Yield 89%. mp: 189–190 °C. ^{1}H NMR (400 MHz, $CDCl_3$) δ (ppm): 2.45 (s, 3H, Ar–CH_3), 3.96 (s, 3H, OCH_3), 3.98 (s, 3H, OCH_3), 7.08 (s, 1H, H-2), 7.28 (d, 1H, J = 8.76 Hz, H-7), 7.58–7.62 (m, 2H, H-4, H-6), 7.80 (d, 1H, J = 7.64 Hz, H-5). ^{13}C NMR (100 MHz, $CDCl_3$) δ: 22.1, 56.4, 118.0, 118.6, 118.8, 119.4, 121.5, 123.9, 133.7, 134.4, 134.7, 145.0, 159.4, 159.6, 182.4, 184.2. IR (KBr, cm^{-1}) 2925, 2854, 1662, 1602, 1236. HRMS (ESI) *m/z*: Calcd for $C_{17}H_{14}O_4Na$ $[M + Na]^+$ 305.0790; found 305.0790.

*4.2.20. 1,8-Diethoxy-3-methylanthracene-9,10-dione (**2b**)*

Yellow solid. Yield 73%. mp: 118–119 °C. ^{1}H NMR (400 MHz, $CDCl_3$) δ (ppm): 1.52 (t, 6H, J = 7.0 Hz, CH_3), 2.43 (s, 3H, Ar–CH_3), 4.17–4.23 (m, 4H, OCH_2), 7.07 (s, 1H, H-2), 7.26 (d, 1H, J = 8.76 Hz, H-7), 7.54–7.61 (m, 2H, H-4, H-6), 7.79 (dd, 1H, J = 7.64, 1.0 Hz, H-5). ^{13}C NMR (100 MHz, $CDCl_3$) δ: 14.6, 14.7, 22.0, 65.3, 118.9, 119.5, 120.2, 122.2, 124.2, 133.5, 134.5, 134.8, 144.8, 158.8, 159.0, 182.3, 184.4. IR (KBr, cm^{-1}) 2926, 2855, 1669, 1601, 1456, 1236. HRMS (ESI) *m/z*: Calcd for $C_{19}H_{18}O_4Na$ $[M + Na]^+$ 333.1103; found 333.1103.

*4.2.21. 1,8-Dipropyloxy-3-methylanthracene-9,10-dione (**2c**)*

Yellow solid. Yield 82%. mp: 112–114 °C. ^{1}H NMR (400 MHz, $CDCl_3$) δ (ppm): 1.12 (t, 6H, J = 7.4 Hz, CH_3), 1.91–1.97 (m, 4H, CH_2) 2.45 (s, 3H, Ar–CH_3), 4.07–4.11 (m, 4H, OCH_2), 7.08 (s, 1H, H-2), 7.26 (d, 1H, J = 7.7 Hz, H-7), 7.57 (t, 1H, J = 8.16 Hz, H-6), 7.63 (s, 1H, H-4), 7.80 (dd, 1H, J = 7.68, 0.92 Hz, H-5). ^{13}C NMR (100 MHz, $CDCl_3$) δ: 10.4, 22.0, 22.5, 71.3, 118.8, 119.7, 119.8, 120.3, 122.3, 124.7, 133.3, 134.6, 134.9, 144.5, 158.9, 159.1, 182.0, 184.5. IR (KBr, cm^{-1}) 2924, 2875, 1671, 1600, 1440, 1233. HRMS (ESI) *m/z*: Calcd for $C_{21}H_{22}O_4Na$ $[M + Na]^+$ 361.1416; found 361.1415.

*4.2.22. 1,8-Dibutoxy-3-methylanthracene-9,10-dione (**2d**)*

Yellow solid. Yield 84%. mp: 97–99 °C. ^{1}H NMR (400 MHz, $CDCl_3$) δ (ppm): 1.02 (t, 6H, J = 7.12 Hz, CH_3), 1.58–1.64 (m, 4H, CH_2), 1.86–1.93 (m, 4H, CH_2), 2.45 (s, 3H, Ar–CH_3), 4.11–4.15 (m, 4H, OCH_2), 7.08 (s, 1H, H-2), 7.26–7.28 (m, 1H, H-7), 7.57 (t, 1H, J = 8.08 Hz, H-6), 7.62 (s, 1H, H-4), 7.80 (d, 1H, J = 7.12 Hz, H-5). ^{13}C NMR (100 MHz, $CDCl_3$) δ: 13.8, 19.2, 22.0, 31.2, 69.5, 118.7, 119.4, 119.6, 120.2, 122.3, 124.7, 133.3, 134.5, 134.8, 144.5, 158.9, 159.0, 182.0, 184.5. IR (KBr, cm^{-1}) 2925, 2855, 1666, 1601, 1323, 1286, 1232, HRMS (ESI) *m/z*: Calcd for $C_{23}H_{26}O_4Na$ $[M + Na]^+$ 389.1729; found 389.1728.

*4.2.23. 1,8-Bis(allyloxy)-3-methylanthracene-9, 10-dione (**2e**)*

Yellow solid. Yield 80%. mp: 106–107 °C. ^{1}H NMR (400 MHz, $CDCl_3$) δ (ppm): 2.45 (s, 3H, Ar–CH_3), 4.73–4.77 (m, 4H, OCH_2), 5.35 (dd, 2H, J = 10.64, 1.32 Hz), 5.63 (dd, 2H, J = 15.6, 1.64 Hz), 6.09–6.13 (m, 2H, CH), 7.09 (s, 1H, H-2), 7.28 (d, 1H, J = 8.0 Hz, H-7), 7.58 (t, 1H, J = 7.76 Hz, H-6), 7.66 (s, 1H, H-4), 7.84 (dd, 1H, J = 7.68, 0.88 Hz, H-5). ^{13}C NMR (100 MHz, $CDCl_3$) δ: 22.0, 70.0, 117.6, 119.2, 119.8, 120.6, 122.2, 124.5, 132.5, 133.4, 133.6, 134.6, 134.9, 144.7, 158.3, 158.5, 182.0, 184.3. IR (KBr, cm^{-1}) 2923, 2855, 1669, 1601, 1586, 1452, 1236, HRMS (ESI) *m/z*: Calcd for $C_{21}H_{18}O_4Na$ $[M + Na]^+$ 357.1103; found 357.1106.

*4.2.24. 1,8-Bis(benzyloxy)-3-methylanthracene-9,10-dione (**2f**)*

Yellow solid. Yield 94%. mp: 183–185 °C. ^{1}H NMR (400 MHz, $CDCl_3$) δ (ppm): 2.45 (s, 3H, Ar–CH_3), 5.31 (s, 4H, OCH_2), 7.16 (s, 1H, H-2), 7.32–7.43 (m, 7H, Ar–H), 7.59 (t, 1H, J = 8.16 Hz, H-6), 7.64–7.69 (m, 5H, Ar–H), 7.86 (dd, 1H, J = 7.72, 0.80 Hz, H-5). ^{13}C NMR (100 MHz, $CDCl_3$) δ: 22.0, 71.1, 119.4, 120.1, 120.3, 120.9, 122.5, 124.8, 126.7, 127.8, 127.8, 128.5, 133.5, 134.6, 134.9, 136.6, 144.8, 158.2, 158.5, 182.0, 184.2. IR (KBr, cm^{-1}) 2922, 2858, 1671, 1600, 1321, 1238, HRMS (ESI) *m/z*: Calcd for $C_{29}H_{22}O_4Na$ $[M + Na]^+$ 457.1416; found 457.1414.

*4.2.25. 1,8-Bis(3-chlorobenzyloxy)-3-methylanthracene-9, 10-dione (**2g**)*

Yellow solid. Yield 70%. mp: 190–192 °C. ^{1}H NMR (400 MHz, $CDCl_3$) δ (ppm): 2.45 (s, 3H, Ar–CH_3), 5.26 (s, 4H, OCH_2), 7.12 (s, 1H, H-2), 7.27–7.37 (m, 5H, Ar–H), 7.58–7.62 (m, 5H, Ar–H), 7.7 (s, 1H, H-4), 7.88 (dd, 1H, J = 7.68, 0.88 Hz, H-5). ^{13}C NMR (100 MHz, $CDCl_3$) δ: 22.0, 70.5, 119.8, 120.4, 120.5, 120.9, 122.4, 124.7, 124.9, 125.0, 126.8, 126.9, 127.9, 128.0, 130.0, 133.7, 134.4, 134.6, 134.9, 138.6, 138.7, 145.1, 158.0, 158.2, 181.9, 183.9. IR (KBr, cm^{-1}) 2922, 2869, 1670, 1601, 1321, 1237. HRMS (ESI) *m/z*: Calcd for $C_{29}H_{20}Cl_2O_4Na$ $[M + Na]^+$ 525.0636; found 525.0634.

*4.2.26. 1,8-Bis(4-iodobenzyloxy)-3-methylanthracene-9, 10-dione (**2h**)*

Yellow solid. Yield 87%. mp: 250–252 °C. ^{1}H NMR (400 MHz, $CDCl_3$) δ (ppm): 2.46 (s, 3H, Ar–CH_3), 5.22 (s, 4H, OCH_2), 7.13 (s, 1H, H-2), 7.30 (d, 1H, J = 8.20, H-7), 7.39–7.42 (m, 4H, Ar–H), 7.61 (t, 1H, J = 8.0 Hz, H-6), 7.70–7.75 (m, 5H, Ar–H), 7.88 (d, 1H, J = 7.56 Hz, H-5). ^{13}C NMR (100 MHz, $CDCl_3$) δ: 22.1, 70.5, 114.0, 119.7, 120.1, 120.3,

120.7, 124.8, 128.7, 128.8, 133.6, 134.6, 134.9, 136.2, 136.3, 137.6, 145.1, 158.0, 158.2, 184.0, 185.7 IR (KBr, cm^{-1}) 2921, 2854, 1665, 1600, 1240. HRMS (ESI) *m/z*: Calcd for $C_{29}H_{20}I_2O_4Na$ $[M + Na]^+$ 708.9349; found 708.9374.

4.2.27. 1,8-Bis(2-bromobenzyloxy)-3-methylanthracene-9, 10-dione: (**2i**)

Yellow solid. Yield 80%. mp: 178–179 °C. ^1H NMR (400 MHz, $CDCl_3$) δ (ppm): 2.50 (s, 3H, Ar–CH_3), 5.28 (s, 4H, OCH_2), 7.20–7.27 (m, 3H, Ar–H), 7.38–7.44 (m, 3H, Ar–H), 7.58–7.67 (m, 3H, Ar–H), 7.71 (s, 1H, H-4), 7.89 (dd, 1H, J = 7.68, 0.52 Hz, H-5), 8.24 (t, 2H, J = 8.2 Hz, Ar–H). ^{13}C NMR (100 MHz, $CDCl_3$) δ: 22.1, 70.3, 70.4, 119.6, 119.7, 120.1, 120.2, 121.1, 122.0, 124.3, 127.8, 128.8, 128.9, 129.0, 132.1, 132.2, 133.8, 134.6, 134.9, 135.9, 136.0, 145.2, 157.9, 158.1, 182.0, 184.09. IR (KBr, cm^{-1}) 2920, 1668, 1600, 1288, 1238. HRMS (ESI) *m/z*: Calcd for $C_{29}H_{20}Br_2O_4Na$ $[M + Na]^+$ 614.9606; found 614.9612.

4.3. Biological evaluation

4.3.1. In vitro COX inhibition assay

The effect of new synthesized compounds on COX-1 and COX-2 were evaluated using COX (ovine) inhibitor screening assay EIA kit according to manufacturer's instructions. Briefly, the compounds were dissolved in dimethylsulfoxide (DMSO). The enzyme COX-1 and COX-2 (10 μL), heme (10 μL) and compounds (20 μL) were added to the supplied reaction buffer solution (950 μL, 0.1 M Tris–HCl, pH 8 containing 5 mM ethylenediamine tetraacetate and 2 mM phenol). The mixture of these solutions was incubated for a period of 10 min at 37 °C, and then COX reactions were initiated by adding arachidonic acid (10 μL, making final concentration 100 μM) solution. The COX reactions were quenched by addition of HCl (1 M, 50 μL) after 2 min and then saturated stannous chloride (100 μL) was added and again incubated for 5 min at room temperature. The $PGF_{2\alpha}$ formed by COX reactions was quantified by EIA. The pre-coated 96-well plate containing compounds was incubated for 18 h at room temperature. After incubation, the plate was washed to remove any unbound reagent and then Ellman's reagent (200 μL), was added followed by incubation for 60 min (until the absorbance of B_o well is in the range 0.3–1.0 A. U.) at room temperature. The plate was then read by an ELISA plate reader at 410 nm.

4.3.2. In vivo assay

Animal study was performed according to the committee for the purpose of control and supervision of experiments on animals (CPCSEA) guidelines and, protocol used in this study was reviewed and approved by Institutional Animal Ethics Committee, NIPER, S.A.S Nagar (IAEC, approval no. IAEC/13/12) [20]. The *in vivo* assessment of compounds was done using the carrageenan-induced rat paw edema method, as described by Winter et al. [21]. Female sprague–dawley rats (180–200 g) were fasted overnight with free access to water prior to experiments and were divided randomly into nine groups (n = 5). Control group received 1 mL of 0.5% hydroxypropyl methylcellulose (HPMC), standard group received 150 μmol/kg of ibuprofen and test groups received 150 μmol/kg of synthesized compounds (**1f–i**, **2e**, **2f** and **2h**). The rats were dosed orally and, after 1 h a subplantar injection of 0.1 mL of 1% solution of carrageenan in sterile distilled water was administered to the left hind footpad of each animal. The paw edema volume was measured with a digital plethysmometer at 0, 3 and 5 h interval after carrageenan injection. Paw edema volume was compared with vehicle control group and percent reduction was calculated as 1-(edema volume in the drug treated group/edema volume in the control group) × 100. Statistically significant differences were determined by one-way ANOVA test followed by Dunnet's t-test.

4.4. Ligand docking procedure

Molecular docking was performed using the GOLD program which uses genetic algorithm and considers full ligand conformational flexibility and partial protein flexibility, i.e., flexibility of side chain residues only [22]. Default docking parameters were used for the docking study which includes 1,00,000 genetic operations on a population size of 100 individuals and mutation rate 95. The crystal structure of COX-1 (pdb id: 3N8Z) and COX-2 (pdb id: 3NT1) having resolution 2.90 Å and 1.73 Å respectively, were taken from the protein data bank (PDB) and considered for the molecular docking study [23]. The COX-1 and COX-2 crystal structures contained flurbiprofen and naproxen as a co-crystal ligand respectively. The docking protocol was set by extracting and re-docking the flurbiprofen and naproxen in the COX-1 and COX-2 crystal structure respectively with a rmsd < 0.60 Å. It was followed by docking of described molecules in the active site defined as 6 Å regions around the co-crystal ligand in the COX-1 and COX-2 protein. Further, all molecules were evaluated for their ADMET properties using the Discovery Studio v 2.5 [24].

Acknowledgments

Authors thank the Director, NIPER for providing financial support and necessary facilities to carry out this work.

Appendix A. Supplementary data

Supplementary data related to this article can be found at http://dx.doi.org/10.1016/j.ejmech.2014.04.033.

References

[1] D.H. Nugteren, E. Hazelhof, Isolation and properties of intermediates in prostaglandin biosynthesis, BBA-Lipid Lipid Met 326 (1973) 448–461.
[2] M. Hamberg, B. Samuelsson, Detection and isolation of an endoperoxide intermediate in prostaglandin biosynthesis, Proceedings of the National Academy of Sciences of the United States of America 70 (1973) 899–903.
[3] A.L. Blobaum, L.J. Marnett, Structural and functional basis of cyclooxygenase inhibition, Journal of Medicinal Chemistry 50 (2007) 1425–1441.
[4] T.D. Warner, J.A. Mitchell, Cyclooxygenases: new forms, new inhibitors, and lessons from the clinic, FASEB Journal: Official Publication of the Federation of American Societies for Experimental Biology 18 (2004) 790–804.
[5] D. Mukherjee, S.E. Nissen, E.J. Topol, Risk of cardiovascular events associated with selective COX-2 inhibitors, JAMA: the Journal of the American Medical Association 286 (2001) 954–959.
[6] R. Gautam, S.M. Jachak, Recent developments in anti-inflammatory natural products, Medicinal Research Reviews 29 (2009) 767–820.
[7] R. Gautam, K.V. Karkhile, K.K. Bhutani, S.M. Jachak, Anti-inflammatory, cyclooxygenase (COX)-2, COX-1 inhibitory, and free radical scavenging effects of *Rumex nepalensis*, Planta Medica 76 (2010) 1564–1569.
[8] R. Gautam, A. Srivastava, S.M. Jachak, Simultaneous determination of naphthalene and anthraquinone derivatives in *Rumex nepalensis* Spreng. Roots by HPLC: comparison of different extraction methods and validation, Phytochemical Analysis 22 (2011) 153–157.
[9] M. Koyama, K. Takahashi, T.C. Chou, Z. Darzynkiewicz, J. Kapuscinski, T.R. Kelly, K.A. Watanabe, Intercalating agents with covalent bond forming capability. A novel type of potential anticancer agents. 2. Derivatives of chrysophanol and emodin, Journal of Medicinal Chemistry 32 (1989) 1594–1599.
[10] K. Bairwa, I.N. Singh, S.K. Roy, J. Grover, A. Srivastava, S.M. Jachak, Rotenoids from *Boerhaavia diffusa* as potential anti-inflammatory agents, Journal of Natural Products 76 (2013) 1393–1398.
[11] C. Selvam, S.M. Jachak, R. Thilagavathi, A.K. Chakraborti, Design, synthesis, biological evaluation and molecular docking of curcumin analogues as antioxidant, cyclooxygenase inhibitory and anti-inflammatory agents, Bioorganic & Medicinal Chemistry Letters 15 (2005) 1793–1797.
[12] R. Gautam, S.M. Jachak, V. Kumar, C.G. Mohan, Synthesis, biological evaluation and molecular docking studies of stellatin derivatives as cyclooxygenase (COX-1, COX-2) inhibitors and anti-inflammatory agents, Bioorganic & Medicinal Chemistry Letters 21 (2011) 1612–1616.
[13] T. Murakami, A. Matsushima, The structure of nepodin, Chemical & Pharmaceutical Bulletin 9 (1961) 654.

[14] R.J. Abraham, M. Mobli, N.M.R. An, IR and theoretical investigation of 1H chemical shifts and hydrogen bonding in phenols, Magnetic Resonance in Chemistry 45 (2007) 865–877.
[15] J. Sorensen, H.F. Clausen, R.D. Poulsen, J. Overgaard, B. Schiott, Short strong hydrogen bonds in 2-acetyl-1, 8-dihydroxy-3, 6-dimethylnaphthalene: an outlier to current hydrogen bonding theory? The Journal of Physical Chemistry A 111 (2007) 345–351.
[16] R.W. Taft, Separation of polar, steric and resonance effects in reactivity, in: M.S. Newman (Ed.), Steric Effects in Organic Chemistry, J. Willey & Sons, New York, 1956, pp. 556–675.
[17] T. Kuroda, F. Suzuki, T. Tamura, K. Ohmori, H. Hosoe, A novel synthesis and potent antiinflammatory activity of 4-hydroxy-2 (1H)-oxo-1-phenyl-1, 8-naphthyridine-3-carboxamides, Journal of Medicinal Chemistry 35 (1992) 1130–1136.
[18] A.S. Kalgutkar, B.C. Crews, S.W. Rowlinson, C. Garner, K. Seibert, L.J. Marnett, Aspirin-like molecules that covalently inactivate cyclooxygenase-2, Science 280 (1998) 1268–1270.
[19] D.J. Huggins, W. Sherman, B. Tidor, Rational approaches to improving selectivity in drug design, Journal of Medicinal Chemistry 55 (2012) 1424–1444.
[20] CPCSEA, guidelines for laboratory animal facility, Indian Journal of Pharmacology 35 (2003) 257–274.
[21] C.A. Winter, E.A. Risley, G.W. Nuss, Carrageenin-induced edema in hind paw of the rat as an assay for antiinflammatory drugs, Experimental Biology and Medicine 111 (1962) 544–547.
[22] G. Jones, P. Willett, R.C. Glen, A.R. Leach, R. Taylor, Development and validation of a genetic algorithm for flexible docking, Journal of Molecular Biology 267 (1997) 727–748.
[23] F.C. Bernstein, T.F. Koetzle, G.J.B. Williams, E.F. Meyer Jr., M.D. Brice, J.R. Rodgers, O. Kennard, T. Shimanouchi, M. Tasumi, The protein data bank: a computer-based archival file for macromolecular structures, Journal of Molecular Biology 112 (1977) 535–542.
[24] Studio, D., Version 2.5, Accelrys. Inc, San Diego, 2009.